



Preparation and Properties of Polymethyl Methacrylate-*b*-polyhedral Oligomeric Silsesquioxane Nanocomposites†

BENHONG YANG*, MENG LI, ZHIJUN HUNG and YUN WU

Department of Chemistry and Materials Engineering, Hefei University, Hefei 230022, P.R. China

*Corresponding author: Fax: +86 551 2158437; Tel: +86 551 2158439; E-mail: yangbh@hfuu.edu.cn

AJC-9540

Inorganic/organic nanocomposites were prepared by blending cage-like methyl methacrylate-modified polyhedral oligomeric silsesquioxane (MMA-POSS) with polymethyl methacrylate (PMMA) in THF solvent. FTIR and ²⁹Si NMR were employed to characterize the structures of the nanocomposites. SEM images showed that the as-prepared films were smooth and no aggregation of MMA-POSS was observed. TGA and DSC results showed that the incorporation of small amount of nanosize MMA-POSS enhanced the thermal stability of PMMA. When 1.0 wt % of MMA-POSS was incorporated into PMMA matrix, the T_g and T_d increased by 16.9 and 21.0 °C, respectively.

Key Words: Nanocomposites, Polyhedral oligomeric silsesquioxane, Polymethyl methacrylate, Thermal properties.

INTRODUCTION

Polyhedral oligomeric silsesquioxane (POSS) is a type of special organosiloxane molecule with general formula (RSiO_{1.5})_n. When n = 8, POSS has a cubic cage-like structure with its eight corners connected with organic groups. Polyhedral oligomeric silsesquioxane is generally considered as the minimal SiO₂ particles because of its 0.53 nm of core size¹. The incorporation of POSS into polymer matrix to form nanocomposites often results in a notable improvement of thermal property of the polymer due to the strong interactions between nanosize POSS and polymer chains. Therefore, POSS/polymer nanocomposites have become a hotspot in materials sciences.

The methods for preparing POSS/polymer nanocomposites can generally be classified into two categories as physical blending²⁻⁴ and chemical copolymerization⁵⁻⁷. The latter one usually takes advantage of the reactive functional groups on POSS corners to copolymerize with organic monomers, ensuring the dispersion of POSS cages at molecular level. The physical blending often fails to achieve due to the easy aggregation of inorganic nanoparticles, however, POSS is special. It could have excellent solubility in some organic solvents because of the corner organic groups. In this paper, the facile solution-blending method was adopted. Polyhedral oligomeric silsesquioxane was previously modified to improve its solubility and then mixed with PMMA in THF to form a homogeneous solution. POSS/PMMA nanocomposites were obtained simply by evaporating the solvent.

EXPERIMENTAL

Octahydridosilsesquioxane (H₈-POSS) was purchased from Amwest Technology Company. Polymethyl methacrylate (Mn ≈ 45000) was bought from Shanghai Reagent Co. Platinum dicyclopentadiene (Pt(dcp), as the catalyst) was synthesized according to the procedures described⁸. Tetrahydrofuran and 1,4-dioxane were dried over 4 Å molecular sieves and distilled from sodium benzophenone ketyl immediately prior to use. All other reagents were used without further purification.

Syntheses of MMA-modified POSS: Methyl methacrylate-modified POSS (MMA-POSS) was synthesized using a standard Schlenk vacuum-line system under a N₂ atmosphere. In brief, 0.425 g of H₈-POSS and 0.4 mg of Pt(dcp) were added in a three-necked flask. The system was degassed and purged with N₂ three times. Anhydrous 1,4-dioxane (20 mL) and MMA (0.96 mL) were injected to dissolve the solid. The hydrosilylation was carried out for 8 h at 80 °C under N₂. The mixture was cooled down to room temperature. The white crystalline powder was filtered out, washed with cyclohexane and recrystallized from tetrahydrofuran/methanol (1:3) to give white crystal powder.

Preparation of MMA-POSS/PMMA nanocomposites: MMA-POSS and polymethyl methacrylate were mixed with polyhedral oligomeric silsesquioxane contents of 0.1, 0.5, 1.0, 2.0 and 4.0 %, respectively and dissolved in THF. After vigorous stirring for 1 h, most THF was driven off and further dried under vacuum.

†Presented to the 4th Korea-China International Conference on Multi-Functional Materials and Application.

Characterization: FTIR spectra were measured with a spectral resolution of 1 cm^{-1} on a Nicolet NEXUS 870 FTIR spectrophotometer using KBr powder at room temperature. ^{29}Si NMR spectra were carried out using a BRUKER AVANCE/DMX 300 spectrometer. SEM images were obtained on a FEI Sirion 400 microscope. Differential scanning calorimetry (DSC) was performed on a TA Instruments DSC 9000 under a continuous nitrogen purge (50 mL/min). The scan rate was $10\text{ }^{\circ}\text{C/min}$ at a temperature range of $30\text{--}300\text{ }^{\circ}\text{C}$. The glass-transition temperature (T_g) was taken as the midpoint of the specific heat increment. Thermogravimetric analyses were carried out using a Perkin-Elmer Pyris 1 thermogravimetric analyzer with a heating rate of $20\text{ }^{\circ}\text{C/min}$ from 30 to $600\text{ }^{\circ}\text{C}$ under a continuous nitrogen purge (100 mL/min). The thermal degradation temperature (T_d) was defined as the temperature of 5% weight lost.

RESULTS AND DISCUSSION

MMA-POSS was synthesized *via* the hydrosilylation reaction between $\text{H}_8\text{-POSS}$ and MMA. Fig. 1 shows the FTIR spectra of $\text{H}_8\text{-POSS}$ and MMA-POSS. Both POSSes show a strong absorption band at *ca.* 1109 cm^{-1} , which is attributed to the characteristic Si–O–Si stretching vibration peak of silsesquioxane cages. Comparing to $\text{H}_8\text{-POSS}$, the Si–H stretching vibration band at 2260 cm^{-1} of MMA-POSS becomes much smaller and C=O stretching vibration band at 1739 cm^{-1} and methylene and methine stretching vibrations at 2960 cm^{-1} and 2870 cm^{-1} appear, indicating that most Si–H on $\text{H}_8\text{-POSS}$ have reacted with C=C on MMA to form MMA-POSS. This is further confirmed by the ^{29}Si NMR spectra of MMA-POSS (Fig. 2). There are two resonance peaks at -67 and -85 ppm , which are respectively ascribed to Si–C and Si–H on POSS. By calculating the peak area ratio, we estimate that about 7.2 Si–H on each $\text{H}_8\text{-POSS}$ cage have been transformed to Si–C, implying that MMA-POSS has been successfully prepared.

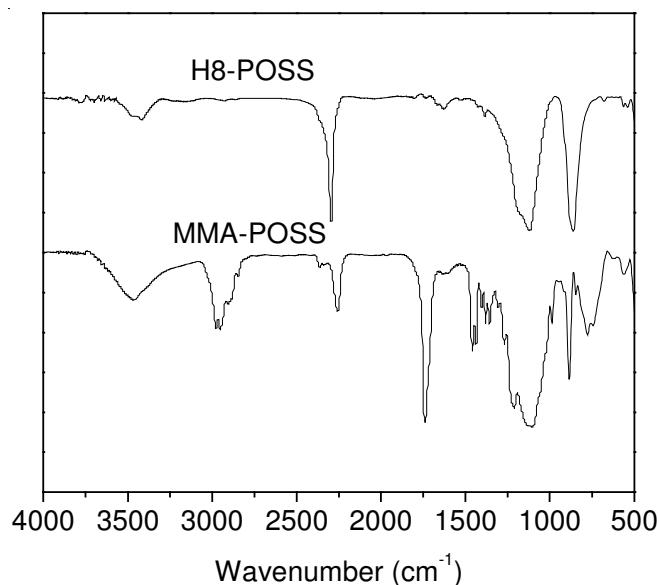


Fig. 1. FTIR spectra of POSS

Fig. 3 indicates the FTIR spectra of MMA-POSS/PMMA. For comparison, FTIR spectra of MMA-POSS and MMA-

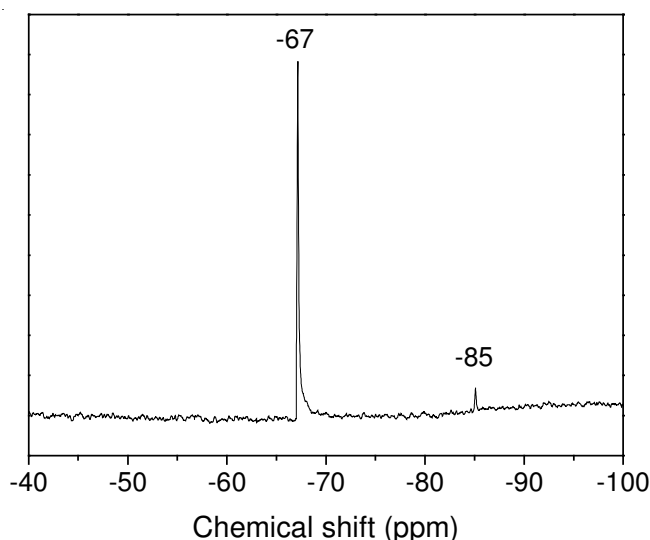


Fig. 2. ^{29}Si NMR spectrum of MMA-POSS

POSS are also showed in Fig. 3. The FTIR spectra of MMA-POSS/PMMA are much similar to that of PMMA, all showing the characteristic absorption bands of PMMA such as C=O stretching vibration peak at 1739 cm^{-1} and methylene and methine stretching vibration bands at 2960 and 2870 cm^{-1} . And meanwhile, the characteristic Si–O–Si stretching vibration peak at *ca.* 1109 cm^{-1} are all observed in the FTIR spectra of MMA-POSS/PMMA nanocomposites and the Si–O–Si peak becomes larger from MMA-POSS/PMMA 0.1% to MMA-POSS/PMMA 4.0% , implying that MMA-POSS has been incorporated into the PMMA matrix and MMA-POSS/PMMA nanocomposites have been successfully prepared.

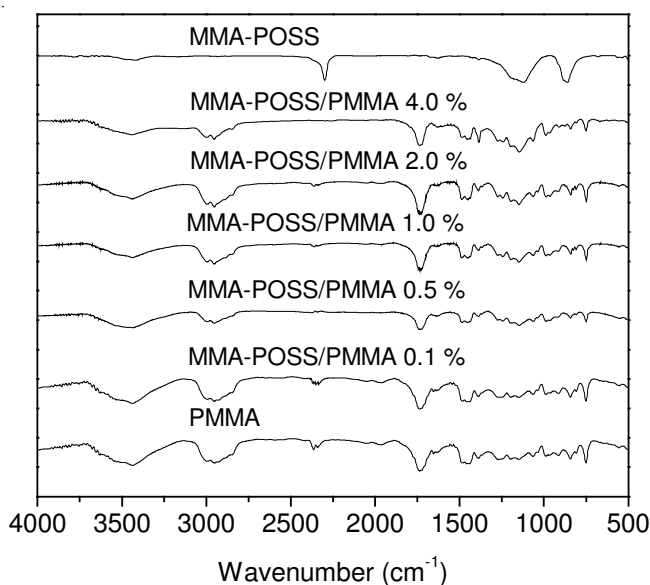


Fig. 3. FTIR spectra of MMA-POSS/PMMA nanocomposites

The successful preparation of MMA-POSS/PMMA nanocomposites is much related to the dispersive state of POSS cages in the PMMA matrix. Fig. 4 shows the SEM images ($\times 5000$) of the thin films of MMA-POSS/PMMA nanocomposites. When MMA-POSS content is relatively low (less than $1.0\text{ wt}\%$), the thin films are rather smooth and MMA-POSS

particles are evenly dispersed. When content is increased to 4.0 %, however, the aggregation of MMA-POSS is observed (Fig. 4C).

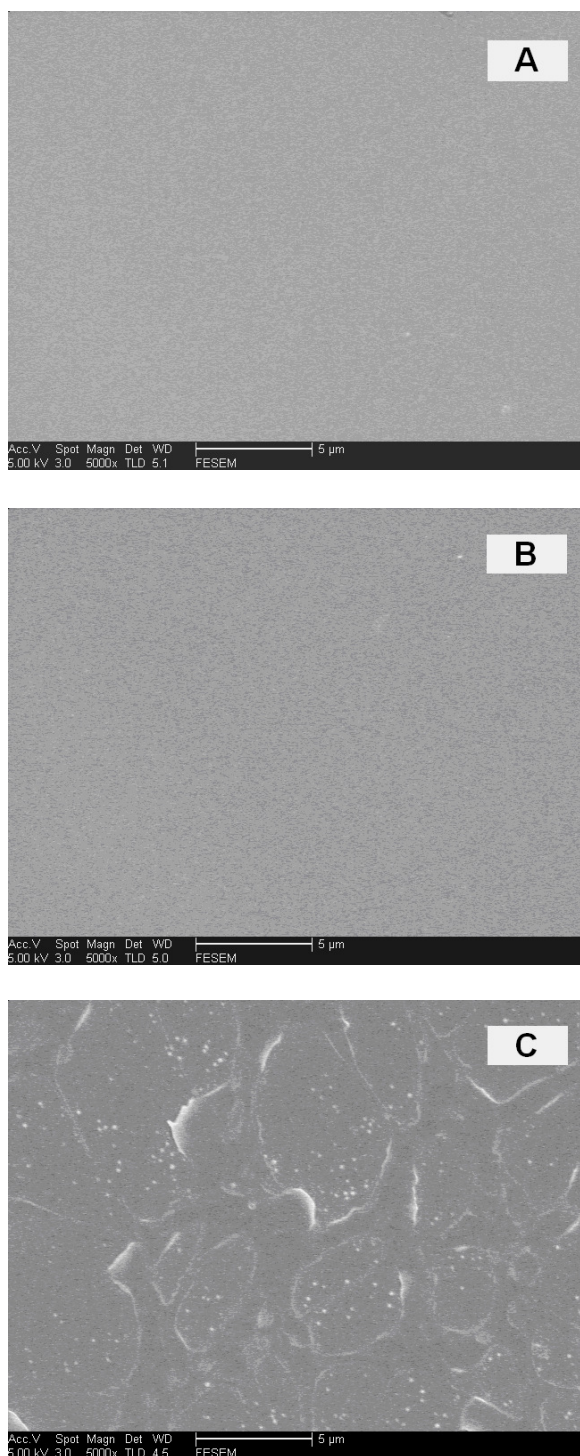


Fig. 4. SEM images of MMA-POSS/PMMA nanocomposites ($\times 5000$): (A) MMA-POSS/PMMA 0.1 %; (B) MMA-POSS/PMMA 1.0 %; (C) MMA-POSS/PMMA 4.0 %

Fig. 5 shows the DSC thermograms of MMA-POSS/PMMA nanocomposites with various POSS contents. For comparison, PMMA homopolymer thermogram is also displayed. As is seen in Table-1, T_g 's of all MMA-POSS/PMMA nanocomposites are higher than that of PMMA

homopolymer. The T_g of the nanocomposite increases gradually with the increase of the POSS contents. For example, the T_g of MMA-POSS/PMMA with 0.1 wt % of POSS (MMA-POSS/PMMA 0.1 %) is 134.7 °C, which is 10.5 °C higher than that (124.2 °C) of the PMMA homopolymer. When content of POSS in the nanocomposite is increased to 1.0 wt %, the T_g reaches as high as 141.1 °C, which is 16.9 °C higher than the T_g of the PMMA homopolymer. With the further increase of POSS content, however, T_g shows a decreasing trend.

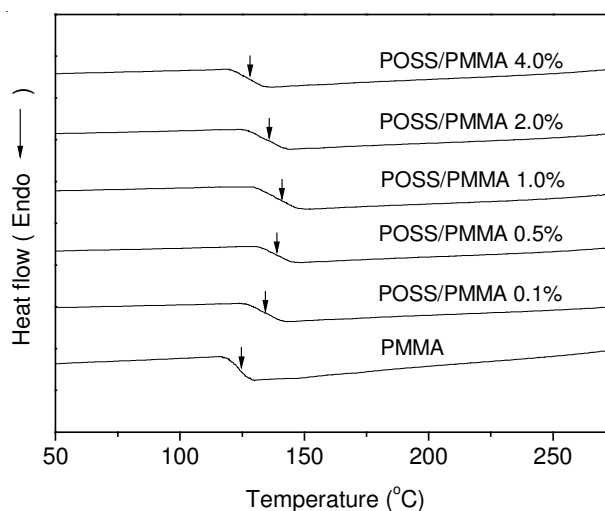


Fig. 5. DSC thermograms of MMA-POSS/PMMA nanocomposites

TABLE-1
THERMAL PROPERTIES OF
MMA-POSS/PMMA NANOCOMPOSITES

Samples	POSS content (wt %)	T_g (°C)	T_d^* (°C)	Char** (%)
PMMA	0.0	124.2	177.2	0.0
MMA-POSS/PMMA (0.1 %)	0.1	134.7	187.2	0.5
MMA-POSS/PMMA (0.5 %)	0.5	139.5	191.3	1.8
MMA-POSS/PMMA (1.0 %)	1.0	141.1	198.2	2.9
MMA-POSS/PMMA (2.0 %)	2.0	135.4	187.2	4.8
MMA-POSS/PMMA (4.0 %)	4.0	126.7	185.8	6.7

*The temperature at 5 % weight loss; **The remained weight at 600 °C.

The T_g of a linear polymer is primarily related to the interaction strength between polymer chains. The T_g 's of MMA-POSS/PMMA nanocomposites differ from that of PMMA implies that the incorporation of MMA-POSS nanoparticles have changed the original interaction strength. When POSS content is less than 1.0 wt %, MMA-POSS cages disperse evenly in the PMMA matrix (Fig. 4A and 4B), enhancing the interactions between POSS cages and PMMA chains due to the strong nanoeffect from POSS. Herein, POSS cages play roles of anchoring points, which restrict the motion of PMMA chains and therefore promote the T_g of MMA-POSS/PMMA nanocomposites. In addition, the polar MMA groups on the surfaces of POSS cages may have strong dipole-dipole interactions with the PMMA chains, providing extra contribution to the increase of T_g . When POSS content is higher than 1.0 wt %, however, the T_g of MMA-POSS/PMMA nanocomposites begins to decrease due to the slight aggregation of POSS cages (Fig. 4C).

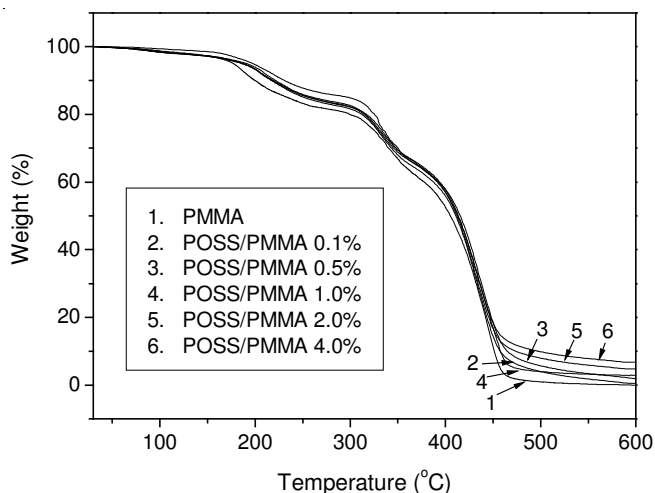


Fig. 6. TGA curves of MMA-POSS/PMMA nanocomposites

Fig. 6 shows the TGA curves of MMA-POSS/PMMA nanocomposites as well as PMMA homopolymer. Pure PMMA shows three-step degradations⁹ at 177.2, 313.6 and 410.6 °C, respectively. Similarly, MMA-POSS/PMMA nanocomposites also indicate three-step degradations, implying that the incorporation of small amount of POSS does not essentially change the thermal properties of PMMA. However, the decomposition temperatures (T_d) of MMA-POSS/PMMA nanocomposites do differ substantially from PMMA. For example, when POSS content is 1.0 wt %, the T_d is 198.2 °C, which is 21.0 °C higher than that of PMMA homopolymer, indicating that incorporation of small amount of POSS into PMMA could improve the thermal stability of PMMA.

Conclusion

(1) A series of MMA-POSS/PMMA nanocomposites were prepared *via* solution-blending method. It reveals that when

small amount of POSS (less than 1.0 wt %) is incorporated into PMMA homopolymer, the thin films of nanocomposites show rather smooth surfaces and POSS cages evenly dispersed in the PMMA matrix.

(2) The thermal properties of MMA-POSS/PMMA nanocomposites are substantially improved due to the strong nanoeffect of POSS and the dipole-dipole interaction between POSS cages and PMMA chains.

(3) Polyhedral oligomeric silsesquioxane (POSS) is a type of inorganic-organic hybrid nanoparticle with its surface bound with eight reactive organic groups, which impart POSS excellent solubility in common solvents, making it possible to produce POSS/Polymer nanocomposites *via* solution-blending process.

ACKNOWLEDGEMENTS

This research was financially supported by the Talents Fund of Hefei University (Grant No. 08RC03).

REFERENCES

1. A. Sellinger and R.M. Laine, *Macromolecules*, **29**, 2327 (1996).
2. N. Hosaka, N. Torikai, H. Otsuka and A. Takahara, *Langmuir*, **23**, 902 (2007).
3. K. Liang, G. Li, H. Toghiani, J.H. Koo and C.U. Pittman, *Chem. Mater.*, **18**, 301 (2006).
4. E.T. Kopesky, G.H. McKinley and R.E. Cohen, *Polymer*, **47**, 299 (2006).
5. H.Y. Xu, B.H. Yang, J.F. Wang, S.Y. Guang and C. Li, *J. Polym. Sci. Part A: Polym. Chem.*, **45**, 5308 (2007).
6. N. Amir, A. Levina and M.S. Silverstein, *J. Polym. Sci. Part A: Polym. Chem.*, **45**, 4264 (2007).
7. A. Lee, J. Xiao and F.J. Feher, *Macromolecules*, **38**, 438 (2005).
8. J. Choi, A.F. Yee and R.M. Laine, *Macromolecules*, **36**, 5666 (2003).
9. J.D. Peterson, S. Vyazovkin and A. Wight, *J. Phys. Chem. B*, **103**, 8087 (1999).